Accelerating Simulations of Cardiac Arrhythmias through Robust Numerical Techniques and Parallel Computing

Guilherme M. Couto[1], **Noemi Z. Monteiro**[1], **Rodrigo W. dos Santos**[1]

[1]Federal University of Juiz de Fora – Juiz de Fora – MG – Brazil

couto.guilherme@engenharia.ufjf.br, nzmonteiro@ice.ufjf.br,

rodrigo.weber@ufjf.edu.br

Abstract. *This paper explores how numerical methods and parallel computing can be used to accelerate simulations of cardiac arrhythmia. The simulations are based on the monodomain cardiac model, governed by a set of partial differential equations (PDEs). The new software could accurately reproduce various types of arrhythmia, such as spiral waves and reentry, by solving the PDEs using an Alternating Direction Implicit (ADI) fractional splitting method. Parallel programming via OpenMP led to a significant reduction in computation time, making the simulations feasible for practical applications.*

1. Introduction

The American Heart Association has reported that cardiovascular diseases were responsible for 27% of the world's total deaths in 2019, highlighting the importance of studying the heart and its mechanisms [Tsao et al. 2022]. Computer and mathematical modeling have played a significant role in the healthcare, including the study of arrhythmias associated with the formation of re-entry waves.

This work couples a cellular ten Tusscher-Noble-Noble-Panfilov model (TNNP) [Ten Tusscher and Panfilov 2006] with the monodomain model and employs Forward Euler (FE) [Strikwerda 2004] and an Alternating Direction Implicit approximation (ADI) [Douglas 1962] with operator-splitting numerical implementations. The results demonstrate that the new scheme based on operator splitting and ADI is robust and faster than the traditional FE. Additionally, the new software was parallelized via OpenMP [OpenMP 2023] and was able to reproduce cardiac arrhythmia, such as spiral wave and re-entry, making it a valuable tool in the study of cardiac mechanisms.

2. Mathematical Methods

2.1. Monodomain model

When in the form of a reaction-diffusion model, the monodomain equations are given by

$$\chi\left(C_m\frac{\partial V}{\partial t}\right)+I_{ion}=\nabla\cdot(\sigma\nabla V)\,,\qquad I_{ion}=g(V,\eta,t),\qquad \frac{\partial \eta}{\partial t}=f(V,\eta,t),\quad (1)$$

where χ is the surface-to-volume ratio of cells (mm^{-1}), C_m is the specific membrane capacitance per unit area (μF mm^{-2}), V is the membrane voltage (mV), η is a vector of state variables, I_{ion} is transmembrane current density (μA mm^{-2}), σ is the conductivity tensor (mS mm^{-1}), and f is a vector-valued function.

2.2. Ten Tusscher-Noble-Noble-Panfilov models

In 2003, was presented a model for human ventricular tissue able to reproduce action potentials of human epicardial, myocardial and endocardial cells. The electrophysiological behavior of a single cell is described by

$$\frac{dV}{dt} = -\frac{1}{C_m}(I_{ion} + I_s), \tag{2}$$

where I_{ion} is the sum of all transmembrane ionic currents and I_s is the density of an imposed stimulus current. The model can be represented by 19 ordinary differential equations. The ionic equations are described in detail in [Ten Tusscher and Panfilov 2006].

The monodomain reaction-diffusion equations coupled to the TNNP model are obtained by applying (2) and the ionic equations in (1), which can be written as

$$\frac{\partial V}{\partial t} = \nabla \cdot (D\nabla V) - \frac{I_{total}}{\chi C_m} \tag{3}$$

$$\frac{\partial \eta}{\partial t} = f(V, \eta, t), \tag{4}$$

where the diffusion coefficient is $D = \frac{\sigma}{\chi}$ and $I_{total} = I_{ion} + I_s$.

The reaction and diffusion part may be separated employing the operator splitting method. In this way, each step consists on solving two problems:

- System of ODEs

$$\frac{\partial V_{i,j}}{\partial t} = -\frac{I_{total}}{\chi C_m} \tag{5}$$

$$\frac{\partial \eta_{i,j}}{\partial t} = f(V_{i,j}, \eta_{i,j}, t). \tag{6}$$

- Parabolic PDE

$$\frac{\partial V_{i,j}}{\partial t} = D\left(\delta_x^2 V_{i,j} + \delta_y^2 V_{i,j}\right), \tag{7}$$

where $\delta_z^2 V_k = \left(V_{k-1} - 2V_k + V_{k+1}\right)/\Delta z^2$ represents a second-order derivative approximation in an arbitrary direction z.

3. Numerical Methods

3.1. Forward Euler

Also known as *explicit Euler*, FE approximates the first-order derivative by progressive differences. In FE scheme with operator splitting, ODEs (5) and (6) respectively become

$$\frac{V_{i,j}^* - V_{i,j}^n}{\Delta t} = -\frac{I_{total}}{\chi C_m} \tag{8}$$

$$\frac{\eta_{i,j}^{n+1} - \eta_{i,j}^n}{\Delta t} = f(V_{i,j}^n, \eta_{i,j}^n, n). \tag{9}$$

And, the PDE (7) becomes

$$\frac{V_{i,j}^{n+1} - V_{i,j}^*}{\Delta t} = D\left(\delta_x^2 V_{i,j}^* + \delta_y^2 V_{i,j}^*\right). \tag{10}$$

3.2. Alternating Direction Implicit Approximation

The basic idea is to apply a dimension splitting of the Laplacian operator to divide the problem into easier one-dimensional problems. In this ADI, the system of ODEs continues to be solved in the same way of the FE, given by (8) and (9). For the PDE, we use an implicit scheme in each direction. Therefore, the PDE (7) is splitted in two parts:

$$\frac{V_{i,j}^{**} - V_{i,j}^{*}}{\Delta t} = D\left(\delta_x^2 V_{i,j}^{**}\right) \tag{11}$$

$$\frac{V_{i,j}^{n+1} - V_{i,j}^{**}}{\Delta t} = D\left(\delta_y^2 V_{i,j}^{n+1}\right). \tag{12}$$

This kind of scheme can also be called local one-dimensional or fractional splitting [Lapidus and Pinder 1999]; in this work, coupled with backward Euler scheme. The method inherits the stability and first-order accuracy from backward Euler. When $\Delta x = \Delta y$ and $\lambda = D\Delta t/\Delta x^2$, Eq. (11) and (12), rearranged, can be rewritten as

$$-\lambda V_{i-1,j}^{**} + (1+2\lambda)V_{i,j}^{**} - \lambda V_{i+1,j}^{**} = V_{i,j}^{*} \tag{13}$$

$$-\lambda V_{i,j-1}^{n+1} + (1+2\lambda)V_{i,j}^{n+1} - \lambda V_{i,j+1}^{n+1} = V_{i,j}^{**}. \tag{14}$$

The resulting linear systems are tridiagonal and can be solved efficiently by Thomas algorithm, so reduced computational cost is an advantage of ADI.

4. Results

Parameters were obtained from benchmark of cardiac tissue electrophysiology simulators [Niederer et al. 2011]. The numerical solutions were obtained for a two-dimensional tissue of 2×2 cm, with $\Delta x = \Delta y = 0.01$ cm, during an interval of 500 ms. Four different time steps were used to compare the two methods. The code was implemented in C and parallelized with *OpenMP*. Simulations were performed in a computer with processor AMD Ryzen 7 3700U 2.30 GHz.

Figure 1 shows a situation with a re-entry wave. Ventricular fibrillation is a dangerous form of arrhythmia caused by breakup of re-entrant waves in cardiac tissue [Weiss et al. 2002]. For that, a second stimulus is applied after the first wave, which initiates the self-sustaining spiral. Figure 2, plotted at t =500 ms, shows that ADI with larger Δt is stable and forms a spiral as well as the FE. Both methods can correctly simulate that arrhythmia. To generate the spiral wave, it was applied a stimulus current of $I_s = -38$ μA at different times and areas. First, at $t = 0$ ms from $x = 0$ cm to $x = 0.04$ cm and along the entire length of y, producing a planar wave front propagating in one direction. The other, at $t = 300$ ms in a square from $x = 0$ cm to $x = 1$ cm and from $y = 0$ cm to $y = 1$ cm, producing a second wave front that curls.

4.1. Methods performance

The errors, stability, whether the spiral was formed and the execution times of each method were analyzed for different Δt. Once there is no analytical solution, each method was compared with its own result with $\Delta t = 0.005$ ms. Metrics for error were Root Mean Square Error (RMSE) and Relative Error - Percentage (REP).

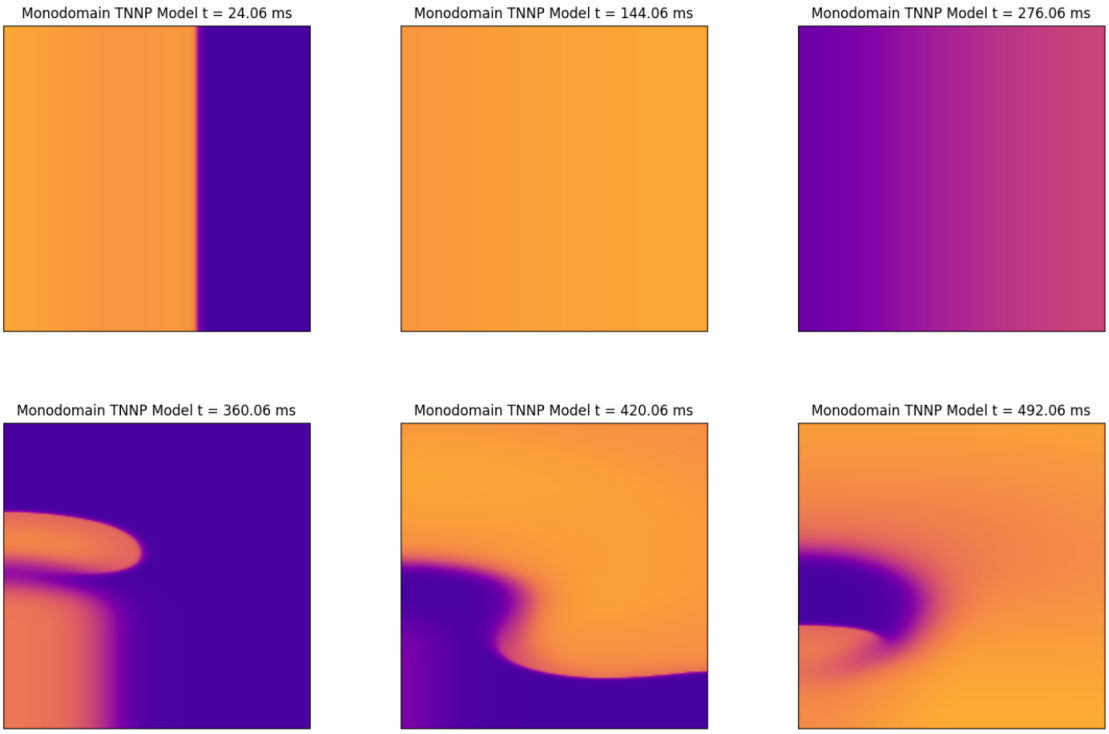

Figure 1. Wave propagation in excitable tissue

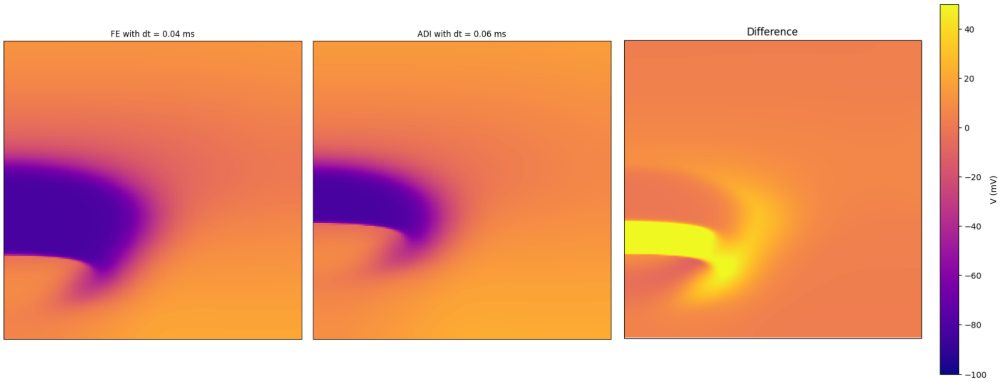

Figure 2. Difference between FE with $\Delta t = 0.04$ ms and ADI with $\Delta t = 0.06$ ms

Tables 1 and 2 show the performance of FE and ADI, respectively, when simulating with 4 threads. In Table 1, lines with no results were consequence of the violation of the Courant–Friedrichs–Lewy (CFL) stability condition [Niederer et al. 2011]. The results presented in Tables 1 and 2 demonstrate that ADI outperformed FE in terms of robustness and speed, reproducing the spiral wave in 408 s compared to 609 s for FE.

The mean times spent to solve ODEs and the PDE are presented in Table 3a (FE) and 3b (ADI), where SV is the standard deviation for three executions. For both methods, it is possible to notice, as shown in [Sachetto Oliveira et al. 2018], that the non-linear part of calculating ODEs, the same for both method, was responsible for the largest portion of the execution time even with the increase of Δt. This is due to the amount and complexity of the calculations that must be done in this step.

Table 1. FE performance

Δt (ms)	RMSE	REP (%)	Spiral	Stability	Exec. Time (s)
0.02	0.66	2.15	Formed	Stable	1174.52
0.04	2.31	7.56	Formed	Stable	609.40
0.06	-	-	Didn't form	Unstable	-
0.08	-	-	Didn't form	Unstable	-

Table 2. ADI performance

Δt (ms)	RMSE	REP (%)	Spiral	Stability	Exec. Time (s)
0.02	4.96	16.41	Formed	Stable	1189.69
0.04	9.83	32.53	Formed	Stable	571.44
0.06	16.19	53.58	Formed	Stable	408.17
0.08	80.61	266.83	Didn't form	Stable	312.98

Table 3. Time to solve ODEs and the PDE

(a) FE times (s)

Δt (ms)	ODEs $\pm$ SV	PDE $\pm$ SV
0.02	1183.17$\pm$16.67	5.86 $\pm$0.12
0.04	591.20 $\pm$10.45	2.92$\pm$0.07

(b) ADI times (s)

Δt (ms)	ODEs $\pm$ SV	PDE $\pm$ SV
0.02	1199.23$\pm$16.85	14.23$\pm$0.10
0.04	584.84 $\pm$15.33	7.15$\pm$0.15
0.06	402.39$\pm$1.06	4.79$\pm$0.02
0.08	305.40$\pm$2.86	3.61$\pm$0.03

The speedups achieved by a parallel algorithm are calculated by dividing the serial execution time by the parallel one. They were calculated with $\Delta t = 0.02$ ms for both methods and presented in Table 4. Parallelization of the software with OpenMP achieved speedups around 2.5, with 4 threads, for both methods.

Table 4. Speed-ups

Number of threads	FE	ADI
1	1.00	1.00
2	1.57	1.59
4	2.54	2.48

5. Conclusion

We implemented the monodomain equation with a ten Tusscher-Noble-Noble-Panfilov model using Forward Euler and an Alternating Direction Implicit method, with serial and parallel execution. ADI has proven to be powerful for applications in cardiac electrophysiology, due to its stability and velocity when compared to FE. The proposed approach can potentially be applied developing new treatments and therapies for heart diseases. Future work can focus on adding biological factors to the model to improve efficacy for clinical applications, while also improving understanding about complexity, sensitivity, and validation. We also propose implement ADI schemes with minor errors, and use a machine with more threads in the future. To the best of our knowledge, this is the first work to apply this ADI fractional splitting method to this type of cardiac behavior and to compare the results with FE.

Acknowledgements. This work was funded by UFJF, Coordenação de Aperfeiçoamento de Pessoal de Nível Superior (CAPES) - Brazil - Finance Code 001, Conselho Nacional de Desenvolvimento Científico e Tecnológico (CNPq), and Empresa Brasileira de Serviços Hospitalares (Ebserh) grant numbers 423278/2021-5 and 315267/2020-8.

References

Douglas, J. (1962). Alternating direction methods for three space variables. *Numerische Mathematik*, 4(1):41–63.

Lapidus, L. and Pinder, G. F. (1999). *Numerical solution of partial differential equations in science and engineering*. John Wiley & Sons.

Niederer, S. A. et al. (2011). Verification of cardiac tissue electrophysiology simulators using an n-version benchmark. *Philosophical Transactions of the Royal Society A: Mathematical, Physical and Engineering Sciences*, 369(1954):4331–4351.

OpenMP (2012-2023). OpenMP Homepage. Last accessed 10 Apr 2023.

Sachetto Oliveira, R., Martins Rocha, B., Burgarelli, D., Meira Jr, W., Constantinides, C., and Weber dos Santos, R. (2018). Performance evaluation of GPU parallelization, space-time adaptive algorithms, and their combination for simulating cardiac electrophysiology. *International journal for numerical methods in biomedical engineering*, 34(2):e2913.

Strikwerda, J. C. (2004). *Finite difference schemes and partial differential equations*. SIAM.

Ten Tusscher, K. H. and Panfilov, A. V. (2006). Alternans and spiral breakup in a human ventricular tissue model. *American Journal of Physiology-Heart and Circulatory Physiology*, 291(3):H1088–H1100.

Tsao, C. W. et al. (2022). Heart disease and stroke statistics—2022 update: a report from the American Heart Association. *Circulation*, 145(8):e153–e639.

Weiss, J. N., Chen, P.-S., Qu, Z., Karagueuzian, H. S., Lin, S.-F., and Garfinkel, A. (2002). Electrical restitution and cardiac fibrillation. *Journal of cardiovascular electrophysiology*, 13(3):292–295.